

Implement of the MPS-FEM Coupled Method for the FSI Simulation of the 3-D Dam-break Problem

Youlin Zhang

State Key Laboratory of Ocean Engineering, School of Naval Architecture, Ocean and Civil Engineering, Shanghai Jiao Tong University, Collaborative Innovation Center for Advanced Ship and Deep-Sea Exploration
Shanghai 200240, China

Decheng Wan*

State Key Laboratory of Ocean Engineering, School of Naval Architecture, Ocean and Civil Engineering, Shanghai Jiao Tong University, Collaborative Innovation Center for Advanced Ship and Deep-Sea Exploration
Shanghai 200240, China

*Corresponding author: dcwan@sjtu.edu.cn

Abstract—In the present study, the coupled moving particle semi-implicit (MPS) method and finite element method (FEM) is developed for the 3-D fluid structure interaction (FSI) problems. Herein, the MPS method is employed for the simulation of fluid domain while the FEM approach is used for the analysis of structural domain. For the implementation of the coupled approach, we proposed a mapping algorithm to transfer quantity values between the particles of flow field and the elements of structural field. In this mapping algorithm, the nonmatching refinement levels of both domains are permitted, which implies that the much larger size of element can be used in the FSI simulation and the computational efficiency can be improved. With the benefit of the proposed MPS-FEM coupled method, the 3-D FSI problem of dam-break flow impacting onto the flexible wall is numerically investigated. The evolutions of free surface and the impacting loads on the wall are compared against those regarding rigid tank. In addition, the deformation and the strength behaviors of the flexible wall are exhibited.

I. INTRODUCTION

The fluid structure interaction (FSI) problems with violent free surface have gained great attentions since they are often encountered in many engineering applications, such as the liquid sloshing in an oil tanker, very large floating structure interacting with waves, flexible structures experiencing dam-break flows, etc. In the past decades, the grid-based methods are much popular in the contributions regarding the simulation of FSI problems. However, it's quite a challenge for such methods to model phenomena that involve complex free surface flows, large deformations of flexible structures. By contrast, the mesh-less methods are free from these difficulties. Therefore, the mesh-less methods, cooperating with the finite element method (FEM), are promising for the FSI problems involving flexible structures and free surface flows.

In the recent decade, several representative mesh-less methods have been proposed for the FSI problems. For instance, the smoothed particle hydrodynamics (SPH) method has been extensively studied and extended to the FSI problems by coupling with the FEM method. Since the SPH method is flexible in describing the violent evolution of the fluid free surface, the movement and the deformation of elastic structures,

Rafiee and Thiagarajan [1] proposed a SPH-based solver for simulation of the dam-break flow interacting with an elastic gate. Liu et al. [2] employed an improved SPH method for modeling the hydro-elastic problems of the water impacting onto a forefront elastic plate. Besides, the particle finite element method (PFEM) is another good candidate for the FSI simulations. In this method, the same Lagrangian formulation is used for both the fluid and the solid analysis, which indicates that a monolithic system of equations could be created for the simultaneous solution of the fluid and structural response. Based on this monolithic approach, Zhu and Scott [3] simulated the process of sloshing wave interacting with a soft beam. In the recent few years, the moving particle semi-implicit (MPS) method, which is originally proposed by Koshizuka and Oka for incompressible flow [4], has also been introduced into the fluid domain analysis of the FSI problems. Hwang et al. [5] employed the MPS method to investigate the sloshing phenomenon in partially filled rectangular tanks with elastic baffles. Zha et al. [6] developed an improved MPS method to solve the hydro-elastic response of a wedge entering calm water. According to these results, the mesh-less methods are of great prospect in the simulation of 2-D FSI problems. However, there are very few works about the application of the mesh-less methods on the 3-D FSI problems.

In the present study, we devote to extend the mesh-less method for 3-D FSI problems. The MPS is employed for the simulation of fluid domain and the FEM method is used for the analysis of structural dynamic response. In the MPS-FEM coupled method, the spaces of fluid domain and structural domain will be dispersed by particles and grids, respectively. Hence, the interface between the fluid boundary particles and structural grids is isomeric and a special technique for the data communication crossing the interface is necessary. Here, a kernel function based interpolation (KFBI) technique is proposed to meet the requirement. The accuracy of the KFBI technique for the force and displacement interpolations between the fluid and the structural domains is validated. Then, the MPS-FEM coupled method is applied to the FSI problem of 3-D dam-break flow interacting with an elastic tank wall, and the influence of structural elasticity on the evolution of violent free surface is comparatively investigated.

II. NUMERICAL METHODS

In the present study, the MPS-FEM coupled method which is a partitioned coupled approach for the FSI problems is developed. Here, the formulas of MPS method, FEM method and the data interpolation on the interface between the fluid and structure domains are briefly introduced.

A. MPS Method for Fluid Analysis

In the MPS method for incompressible viscous flow, the governing equations which include the continuity equations and the Navier-Stokes equations, should be expressed by the particle interaction models based on the kernel function. Here, the kernel function presented by Zhang et al. [7] is employed.

$$W(r) = \begin{cases} \frac{r_e}{0.85r + 0.15r_e} - 1 & 0 \leq r < r_e \\ 0 & r_e \leq r \end{cases} \quad (1)$$

where r is distance between particles and r_e is the effect radius.

The particle interaction models, including the differential operators of gradient, divergence and Laplacian, are defined as

$$\langle \nabla \phi \rangle_i = \frac{\dim}{n^0} \sum_{j \neq i} \frac{\phi_j + \phi_i}{|\mathbf{r}_j - \mathbf{r}_i|^2} (\mathbf{r}_j - \mathbf{r}_i) \cdot W(|\mathbf{r}_j - \mathbf{r}_i|) \quad (2)$$

$$\langle \nabla \cdot \boldsymbol{\Phi} \rangle_i = \frac{\dim}{n^0} \sum_{j \neq i} \frac{(\boldsymbol{\Phi}_j - \boldsymbol{\Phi}_i) \cdot (\mathbf{r}_j - \mathbf{r}_i)}{|\mathbf{r}_j - \mathbf{r}_i|^2} W(|\mathbf{r}_j - \mathbf{r}_i|) \quad (3)$$

$$\langle \nabla^2 \phi \rangle_i = \frac{2\dim}{n^0 \lambda} \sum_{j \neq i} (\phi_j - \phi_i) \cdot W(|\mathbf{r}_j - \mathbf{r}_i|) \quad (4)$$

where ϕ is an arbitrary scalar function, $\boldsymbol{\Phi}$ is an arbitrary vector, \dim is the number of space dimensions, n^0 is the initial particle number density for incompressible flow, λ is a parameter defined as

$$\lambda = \frac{\sum_{j \neq i} W(|\mathbf{r}_j - \mathbf{r}_i|) \cdot |\mathbf{r}_j - \mathbf{r}_i|^2}{\sum_{j \neq i} W(|\mathbf{r}_j - \mathbf{r}_i|)} \quad (5)$$

which is introduced to keep the variance increase equal to that of the analytical solution [4].

In the present MPS method, the pressure Poisson equation (PPE) with the mixed source term is employed to satisfy the incompressible condition of fluid domain and defined as

$$\langle \nabla^2 P^{n+1} \rangle_i = (1 - \gamma) \frac{\rho}{\Delta t} \nabla \cdot \mathbf{V}_i^* - \gamma \frac{\rho}{\Delta t^2} \frac{\langle n^* \rangle_i - n^0}{n^0} \quad (6)$$

where γ is a blending parameter with a value between 0 and 1. The range of $0.01 \leq \gamma \leq 0.05$ is better according to numerical experiments conducted by Lee et al. [8] In this paper, $\gamma=0.01$ is adopted for all the simulations.

B. Structure Solver Based on the FEM Method

In the FEM method, the deformation of structure is governed by the dynamic equations expressed as

$$\mathbf{M} \ddot{\mathbf{y}} + \mathbf{C} \dot{\mathbf{y}} + \mathbf{K} \mathbf{y} = \mathbf{F}(t) \quad (7)$$

$$\mathbf{C} = \alpha_1 \mathbf{M} + \alpha_2 \mathbf{K} \quad (8)$$

where \mathbf{M} , \mathbf{C} , \mathbf{K} are the mass matrix, the Rayleigh damping matrix, the stiffness matrix of the structure, respectively. \mathbf{F} is the external force vector acting on structure, and varies with computational time. \mathbf{y} is the displacement vector of structure. α_1 and α_2 are coefficients which are related with natural frequencies and damping ratios of structure.

To solve the structural dynamic equations, another two group functions should be supplemented to set up a closed-form equation system. Here, Taylor's expansions of velocity and displacement developed by Newmark [9] are employed:

$$\dot{\mathbf{y}}_{t+\Delta t} = \dot{\mathbf{y}}_t + (1 - \gamma) \ddot{\mathbf{y}}_t \Delta t + \gamma \ddot{\mathbf{y}}_{t+\Delta t} \Delta t, \quad 0 < \gamma < 1 \quad (9)$$

$$\mathbf{y}_{t+\Delta t} = \mathbf{y}_t + \dot{\mathbf{y}}_t \Delta t + \frac{1 - 2\beta}{2} \ddot{\mathbf{y}}_t \Delta t^2 + \beta \ddot{\mathbf{y}}_{t+\Delta t} \Delta t^2, \quad 0 < \beta < 1 \quad (10)$$

where β and γ are important parameters of the Newmark method, and selected as $\beta=0.25$, $\gamma=0.5$ for all simulations in present paper. The nodal displacements at $t=t+\Delta t$ can be solved by the following formulas [10]:

$$\bar{\mathbf{K}} \mathbf{y}_{t+\Delta t} = \bar{\mathbf{F}}_{t+\Delta t} \quad (11)$$

$$\bar{\mathbf{K}} = \mathbf{K} + a_0 \mathbf{M} + a_1 \mathbf{C} \quad (12)$$

$$\begin{aligned} \bar{\mathbf{F}}_{t+\Delta t} = & \mathbf{F}_t + \mathbf{M}(a_0 \mathbf{y}_t + a_2 \dot{\mathbf{y}}_t + a_3 \ddot{\mathbf{y}}_t) \\ & + \mathbf{C}(a_1 \mathbf{y}_t + a_4 \dot{\mathbf{y}}_t + a_5 \ddot{\mathbf{y}}_t) \end{aligned} \quad (13)$$

$$a_0 = \frac{1}{\beta \Delta t^2}, \quad a_1 = \frac{\gamma}{\beta \Delta t}, \quad a_2 = \frac{1}{\beta \Delta t},$$

$$a_3 = \frac{1}{2\beta} - 1, \quad a_4 = \frac{\gamma}{\beta} - 1, \quad (14)$$

$$a_5 = \frac{\Delta t}{2} \left(\frac{\gamma}{\beta} - 2 \right), \quad a_6 = \Delta t (1 - \gamma), \quad a_7 = \gamma \Delta t$$

where $\bar{\mathbf{K}}$ and $\bar{\mathbf{F}}$ are the so-called effective stiffness matrix and effective force vector, respectively. Finally, the accelerations and velocities corresponding to the next time step are updated as follows.

$$\ddot{\mathbf{y}}_{t+\Delta t} = a_0(\mathbf{y}_{t+\Delta t} - \mathbf{y}_t) - a_2\dot{\mathbf{y}}_t - a_3\ddot{\mathbf{y}}_t \quad (15)$$

$$\dot{\mathbf{y}}_{t+\Delta t} = \dot{\mathbf{y}}_t + a_6\ddot{\mathbf{y}}_t + a_7\ddot{\mathbf{y}}_{t+\Delta t} \quad (16)$$

C. KFBI Technique for Data Interpolation

For the simulation of 3D FSI problems based on aforementioned MPS-FEM coupled method, the space of fluid domain will be dispersed by particles while the space of structural domain will be dispersed by grids. In general, the fine particles should be arranged within the fluid domain to keep a satisfactory precision for the fluid analysis. By contrast, the much coarser grids could be accurate enough for the structure analysis, which indicates that the fluid particles are usually not coincided with the structural nodes on the interface between the fluid and structure domain, as shown as Figure 1. Hence, the isomeric interface between the two domains may result in the challenge of data exchange in the process of FSI simulation. In the present study, the kernel function based interpolation technique is proposed to apply the external force carried by the fluid particles onto the structural nodes and update the positions of boundary particles corresponding to the displacements of structural nodes.

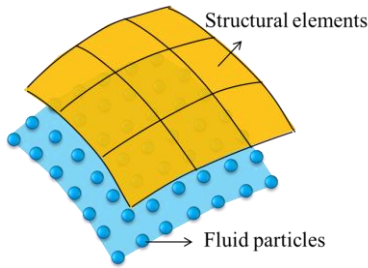


Figure 1. Interface between the fluid and structure domains

The schematic diagram of the KFBI technique for the force transformation from the fluid domain to the structural boundary is shown in Figure 2. In the KFBI technique, the boundary particle of the fluid domain will be denoted as the neighbour particle of the structure node while the distance between the particle and the node is smaller than the effect radius r_{ei} of interpolation. The weighted value of the fluid force of the neighbour particle $W(|\mathbf{r}_i - \mathbf{r}_n|)$ is calculated based on (1). Then, the equivalent nodal force F_n corresponding to the node n is obtained by the summation of force components regarding to the neighbour particles.

$$F_n = \frac{\sum_i P_i \cdot l_0^2 \cdot W(|\mathbf{r}_i - \mathbf{r}_n|)}{\sum_i W(|\mathbf{r}_i - \mathbf{r}_n|)} \quad (17)$$

where P_i is the pressure of the boundary particle obtained from the fluid domain, l_0 is the initial distance between the neighbour particles.

The schematic diagram of the technique for the deformation of the fluid structure interface is shown in Figure 3. The fluid boundary which is consisted of particles will deform corresponding to the deformation of structural boundary. The deflection value of boundary particle w_m can be obtained by the interpolation based on the kernel functions $W(|\mathbf{r}_i - \mathbf{r}_m|)$ and the nodal displacement δ_i .

$$w_m = \frac{\sum_i \delta_i \cdot W(|\mathbf{r}_i - \mathbf{r}_m|)}{\sum_i W(|\mathbf{r}_i - \mathbf{r}_m|)} \quad (18)$$

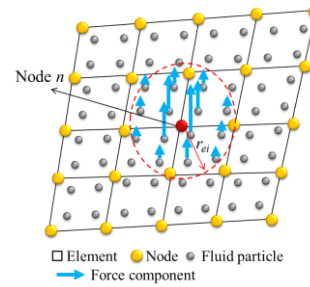


Figure 2. Schematic diagram of the force interpolation

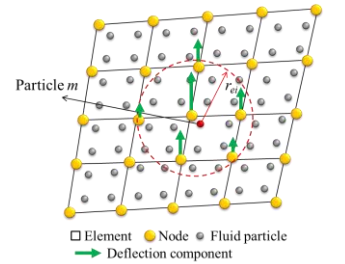


Figure 3. Schematic diagram of the displacement interpolation

III. NUMERICAL VALIDATION

In this paper, a FSI solver, which includes the fluid domain calculation module, the structural domain calculation module and the interface data interpolation module, is developed based on the partitioned coupling strategy. For the fluid simulation, the accuracy of the fluid domain calculation module has been validated by a series of benchmarks in the previous works of our study group [7][11][12][13][14]. Here, the objective of the study in the present section is to validate the reliability of the other two modules.

A. Validation of Structural Domain Calculation Module

For the validation of the structural domain calculation module, the numerical test of the response of a square sheet is carried out. The schematic diagram of geometric dimensions of the square sheet is shown as the Figure 4. The side length and the thickness of the sheet are 2 m, 0.001 m, respectively. The sheet is clamped at all the four edges and dispersed by quadrilateral elements with size of 0.1 m. The concentrated force $F(t)=10$ N is applied at the geometric center A of the plate in the normal direction. The detailed calculation parameters can be found in the Table I.

TABLE I. PARAMETERS FOR STRUCTURAL RESPONSE TEST

Structural parameters	Values
Structure density (kg/m ³)	1800
Young's modulus (GPa)	40
Poisson's ratio	0.3
Element size (m)	0.1
Damping coefficients α_1	0.0
Damping coefficients α_2	0.0
Time step size (s)	1×10^{-3}

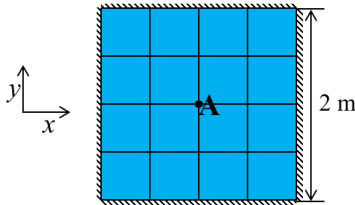


Figure 4. Schematic diagram of the square plane

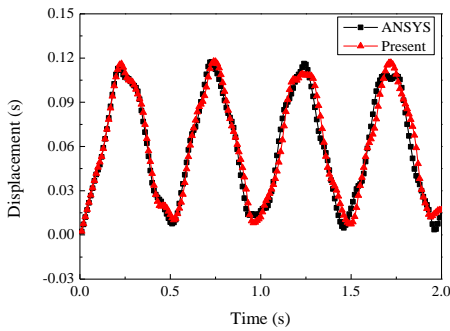


Figure 5. Time history of the displacement at the center of the square plane

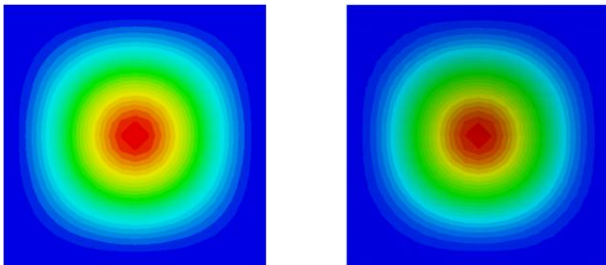


Figure 6. Deformations of the square plane at $t=0.75$ s (Left: ANSYS, right: present result)

Figure 5 shows the time histories of structural vibration at the geometric center A of the plate. Good agreement between the results from the present structural domain calculation module and the ANSYS software can be observed. Furthermore, the structural deformation contour at the time 0.75 s is compared against that calculated by the ANSYS software, as shown in the Figure 6. It can be noticed that the consistent deformation form is obtained by the two structure solver, which indicates that the structural domain calculation module of the present solver is reliable and can be applied to the structural dynamic response analysis of the FSI problems.

B. Validation of Data Interpolation Module

To validate the interpolation accuracy of the interface data transformation module, two numerical tests are carried out in the present section. The accuracy of the fluid force transformation from the fluid domain to the structural domain will be investigated by the first test. In this test, the rectangular sheet, which is with the length of 2 m and width of 0.6 m, is dispersed by the fluid particles and the structural elements, respectively. The distance between neighbour particles is 0.02 m and the size of element is 0.05 m. The triangular distributed force in the normal direction is applied onto the particle model of the rectangular sheet, as shown in the Figure 7. The value of force carried by the particles is calculated by

$$F=1000-500x \quad (19)$$

With the help of the interface data interpolation module, the force on the particle model can be transferred to the nodes of the element model. Figure 8 shows the force distribution on the element model. It can be noticed that the present maximum 2.493 N approximates to the theoretical value 2.5 N.

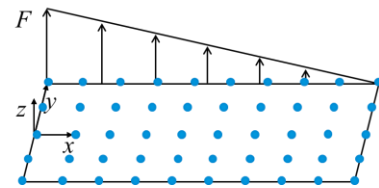


Figure 7. Diagrammatic sketch of force distribution on the particle model

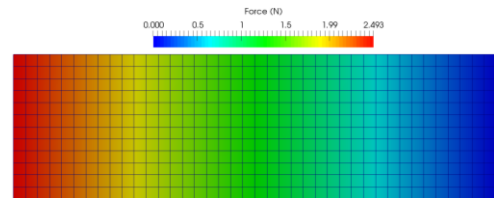


Figure 8. Force distribution on the element model

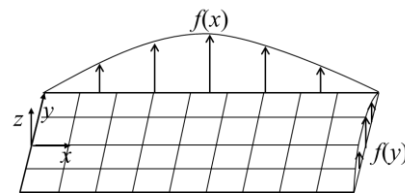


Figure 9. Diagrammatic sketch of deformation of the element model

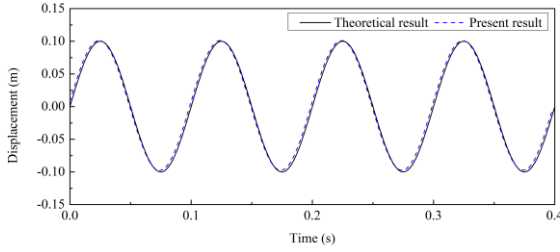


Figure 10. Displacement of the geometric center point of the particle model

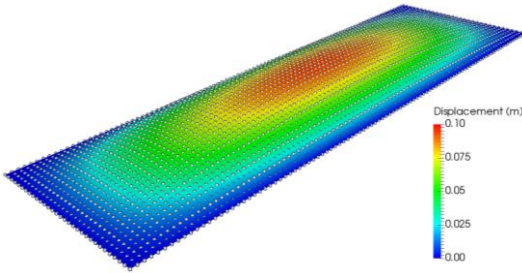


Figure 11. Deformation of the particle model ($t=0.12$ s)

In the second test, the accuracy of the deformation of the fluid boundary in accordance with that of the structural boundary is investigated. The rectangular sheet is dispersed to the same particle and element models. The structural boundary is forced to deform by setting the nodal velocity of the element model. As shown in Figure 9, the structural node will move in the normal direction and the distributed nodal velocity performs the parabolic shape in both x and y directions. The nodal velocity can be calculated by

$$V = 2\pi f(x)f(y)\cos(\omega t)$$

$$\text{where } f(x) = 2x - x^2, f(y) = 1 - \frac{100}{9}y^2 \quad (20)$$

By the interface data interpolation module, the deformation values of the boundary particles can be obtained. Figure 10 shows the present interpolation value of the deflection on the geometric center point of the particle model and the theoretical value of the structure nodal displacement. Good agreement can be achieved between the two results. Furthermore, the deformed particle model and element model are compared at time 0.12 s, as shown in Figure 11. It can be found that the shapes of the two models are coincident with each other.

According to the results of the two tests, we deem that the interface data interpolation module is accurate in force and deformation value interpolation between the fluid and the structure domains.

IV. NUMERICAL SIMULATIONS

A. Numerical Setup

In this section, the numerical simulation of the fluid structure interaction between the dam-break slamming wave and the elastic wall is carried out. The applicability of the MPS-FEM coupled method in the 3-D fluid structure interaction problem is investigated. Figure 12 shows the schematic diagram of the computational model. All the walls of the tank are rigid except the right one. Elastic material is used for the right wall of the tank and the four edges of the wall are clamped on the adjacent walls. A pressure measuring point is mounted at the midpoint P of the bottom of the elastic wall, and five displacement measuring points (A-E) are arranged above the point P with the spacing of 0.1 m. Detailed parameters of the material property and the numerical condition are shown in Table II.

TABLE II. FLUID AND STRUCTURAL PARAMETERS OF SIMULATION

	Parameters	Values
Fluid	Fluid density (kg/m^3)	1000
	Kinematic viscosity (m^2/s)	1×10^{-6}
	Gravitational acceleration (s/m^2)	9.81
	Particle spacing (m)	0.03
	Number of fluid particles	15200
	Total number of particles	44371
	Time step size (s)	1×10^{-4}
Structure	Structure density (kg/m^3)	1800
	Young's modulus (GPa)	10
	Poisson's ratio	0.3
	Element size (m)	0.01
	Damping coefficients α_1	0.025
	Damping coefficients α_2	0.0005
	Time step size (s)	1×10^{-4}

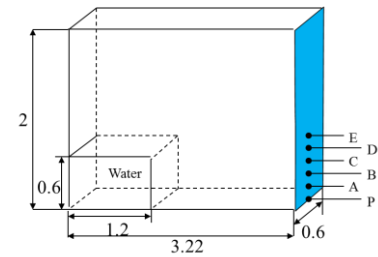


Figure 12. Schematic diagram of the computational model (Unit:m)

B. Numerical Results

To investigate the effect of structural elasticity to the evolution of free surface, the dam-break flows in both rigid tank and elastic tank are numerical simulated. Figure 13 shows the comparison of free surfaces in the rigid tank and the elastic tank at four instants. At the time 0.8 s, the upward jet flow is generated after the dam-break flow impacting onto the right wall of the tank. The height of jet flow in the elastic tank is slightly lower than that in the rigid tank. At the instant 1.4 s, the water front of jet flow falls down and the water surface with the rolling shape is formed. It can be noticed that the shape of rolling water surface approximates circular arc in the rigid tank, while that is closed to an

elliptical arc in the elastic tank. In addition, more the splashed water particles in the rigid tank are observed than those in the elastic tank. It may induced by the energy dissipation during the deformation of the lateral wall. At the instant 1.6 s, an air bubble is generated after the rolling of water front. As shown in the side view, the bubble in the elastic tank presents irregular three-dimensional shape while that in the rigid tank presents the two-dimensional characteristic. At the time 1.9 s, the water particles near the elastic wall are bounced back into the tank during the vibration of the structure, and the separation between the water and the wall is formed.

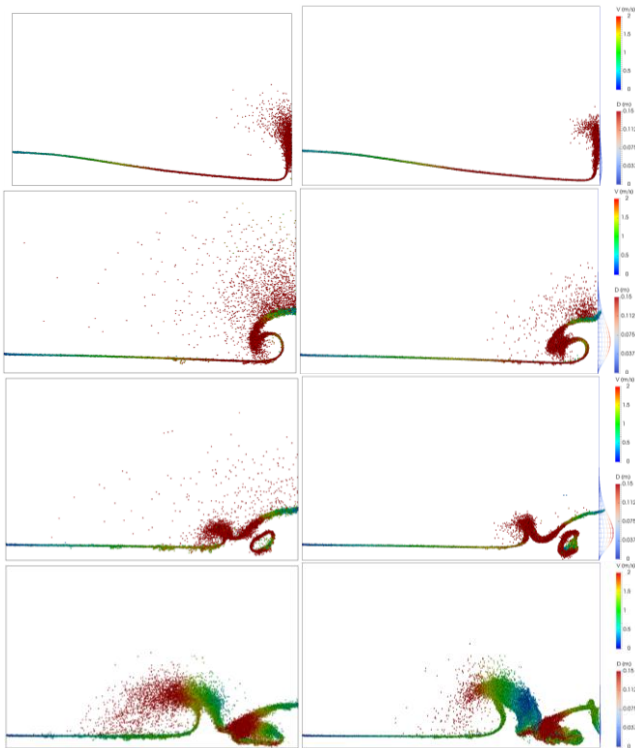


Figure 13. Evolution of free surface in side view (from top to bottom: $t=0.8, 1.4, 1.6, 1.9$ s)

Figure 14 shows the time histories of the structural vibration at the five measuring points on the elastic wall. It can be noticed that the trends of the curves are similar to each other except the peak values of the vibration. At the time 0.62 s, the dam-break wave reaches the right end of the tank and the elastic wall starts to deform due to the impact load. As more and more water particles acting onto the elastic wall, the amplitudes of the deformation increase and reach to the maximums at the instant 1.6 s. In the following stage, the elastic wall vibrates with the decreasing amplitudes since the combined action of the fluid load and the structural damping force. Besides, the elastic wall vibrates with the maximum amplitude in the transverse direction at the measuring point C which is 0.3 m above the bottom of the tank.

In the Figure 15, the time histories of impact loads at the measuring point P are compared between the elastic tank and the rigid tank. At the initial instant ($t=0.62$ s) of the

impact phenomenon, the first peak value of pressure on the lateral wall of the elastic tank is 9225 Pa, which is 21% smaller than that regarding the rigid tank (11673 Pa). And at the instant $t \approx 1.56$ s, which is close to the time that the largest amplitude of structural deformation occurs, the second peak of pressure is observed. In the following stage, the pressure history acting on the elastic wall presents significant fluctuation which is similar with the trend of structural vibration. It could be inferred that the varying of impact load acting on the wall is more complex since the vibration of the tank wall.

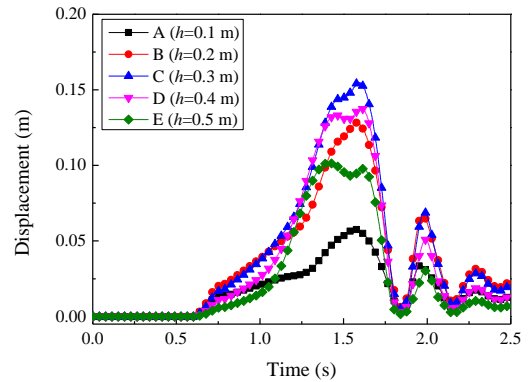


Figure 14. Time histories of vibrations on the elastic wall

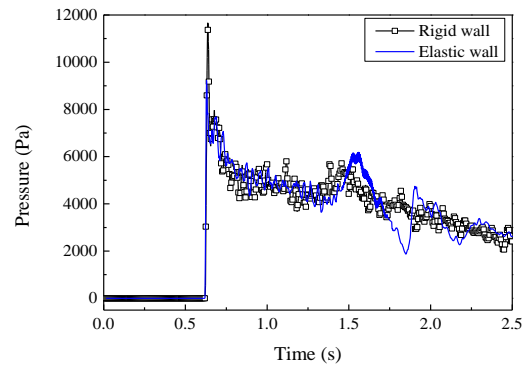


Figure 15. Time histories of impact loads at the measuring point P

V. CONCLUSIONS

In the present study, the MPS-FEM coupled method is developed for 3-D FSI problems. The kernel function based interpolation (KFBI) technique is proposed for the data transformation on the interface between the fluid and structural domains. To validate the reliability of the structural domain calculation module, the numerical test of the vibration response of a square sheet under the constant force is carried out. Both the time history of structural vibration and the deformation form of the sheet are in good agreements with the results calculated by the ANSYS software. Then, the interpolation accuracy of the KFBI technique is validated by two numerical tests. Coincident quantities of force and structural deformation can be achieved between the fluid boundary and the structural boundary. Finally, the MPS-FEM coupled solver is used to simulate the interaction between the dam-break flow and the

elastic wall. Different phenomena of the dam-break flow can be observed in the elastic tank. For instance, the qualitative results show that the evolutions of free surface in the elastic tank present obviously three dimensional characters in comparison with those of rigid tank. The quantitative results show that the impulse pressure induced by the dam-break wave impacting onto the elastic wall is 21% smaller than that regarding the rigid tank. In summary, as a preliminary attempt, present study develops a fully Lagrangian FSI approach and shows the capability of the in-house solver in simulation the 3-D FSI problems with violent free surface.

ACKNOWLEDGEMENT

This work is supported by the National Natural Science Foundation of China (51379125, 51490675, 11432009, 51579145), Chang Jiang Scholars Program (T2014099), Shanghai Excellent Academic Leaders Program (17XD1402300), Program for Professor of Special Appointment (Eastern Scholar) at Shanghai Institutions of Higher Learning (2013022), Innovative Special Project of Numerical Tank of Ministry of Industry and Information Technology of China (2016-23/09) and Lloyd's Register Foundation for doctoral student, to which the authors are most grateful.

REFERENCES

- [1] A. Rafiee and K. P. Thiagarajan, "An SPH projection method for simulating fluid-hypoelastic structure interaction," *Comput. Methods Appl. Mech. Eng.*, vol. 198, pp. 2785–2795, 2009.
- [2] M. B. Liu, J. R. Shao, and H. Q. Li., "Numerical simulation of hydro-elastic problems with smoothed particle hydrodynamics method," *Journal of Hydrodynamics, Ser. B*, vol. 25(5), pp.673–682, 2013.
- [3] M. J. Zhu and M. H. Scott, "Direct differentiation of the quasi-incompressible fluid formulation of fluid–structure interaction using the PFEM," *Computational Particle Mechanics*, vol. 4(3), pp. 1–13, 2016.
- [4] S. Koshizuka and Y. Oka, "Moving particle semi-implicit method for fragmentation of incompressible fluid," *Nuclear Science and Engineering*, vol. 123, pp. 421–434, 1996.
- [5] S. C. Hwang, J. C. Park, H. Gotoh, A. Khayyer, and K. J. Kang, "Numerical simulations of sloshing flows with elastic baffles by using a particle-based fluid–structure interaction analysis method," *Ocean Engineering*, vol. 118, pp. 227–241, 2016.
- [6] R. S. Zha, H. Peng, and W. Qiu, "Solving 2D coupled water entry problem by an improved MPS method," *The 32nd International Workshop on Water Waves and Floating Bodies*, Dalian, China, pp. 23–26, April, 2017.
- [7] Y. X. Zhang, D. C. Wan, and T. Hino, "Comparative study of MPS method and level-set method for sloshing flows," *Journal of hydrodynamics*, vol. 26(4), pp. 577–585, 2014.
- [8] B. H. Lee, J. C. Park, M. H. Kim, S. J. Jung, M. C. Ryu, and Y. S. Kim, "Numerical simulation of impact loads using a particle method," *Ocean Engineering*, vol. 37, pp. 164–173, 2010.
- [9] N. M. Newmark, "A method of computation for structural dynamics," *Journal of the engineering mechanics division*, vol. 85(3), pp. 67–94, 1959.
- [10] K. M. Hsiao, J. Y. Lin, and W. Y. Lin, "A consistent co-rotational finite element formulation for geometrically nonlinear dynamic analysis of 3-D beams," *Comput. Methods Appl. Mech. Engrg*, vol. 169, pp. 1–18, 1999.
- [11] Y. L. Zhang, X. Chen, and D. C. Wan, "MPS-FEM coupled method for the comparison study of liquid sloshing flows interacting with rigid and elastic baffles," *Applied Mathematics and Mechanics*, vol. 37(12), pp. 1359-1377, 2016.
- [12] Y. L. Zhang, Z. Y. Tang, and D. C. Wan, "Numerical investigations of waves interacting with free rolling body by modified MPS method," *International Journal of Computational Methods*, vol. 13(4), pp. 1641013-1–1641013-14, 2016.
- [13] Z. Y. Tang, Y. L. Zhang, and D. C. Wan, "Multi-resolution MPS method for free surface flows," *International Journal of Computational Methods*, vol. 13 (4), pp. 1641018-1–1641018-17, 2016.
- [14] Y. L. Zhang and D. C. Wan, "Numerical study of interactions between waves and free rolling body by IMPS method," *Computers and Fluids*, vol. 155, pp.124–133, 2017.